UNIVERSITY OF BIRMINGHAM
University of Birmingham Research at Birmingham

Macroevolutionary trends in theropod dinosaur feeding mechanics

Ma, Wai Sum; Pittman, Michael; Butler, Richard; Lautenschlager, Stephan

DOI:
10.1016/j.cub.2021.11.060

License:
Creative Commons: Attribution-NonCommercial-NoDerivs (CC BY-NC-ND)

Document Version
Peer reviewed version

Citation for published version (Harvard):
Ma, WS, Pittman, M, Butler, R & Lautenschlager, S 2022, 'Macroevolutionary trends in theropod dinosaur feeding mechanics', *Current Biology*, vol. 32, no. 3, pp. 677-686.e3. https://doi.org/10.1016/j.cub.2021.11.060

Link to publication on Research at Birmingham portal

General rights
Unless a licence is specified above, all rights (including copyright and moral rights) in this document are retained by the authors and/or the copyright holders. The express permission of the copyright holder must be obtained for any use of this material other than for purposes permitted by law.

•Users may freely distribute the URL that is used to identify this publication.
•Users may download and/or print one copy of the publication from the University of Birmingham research portal for the purpose of private study or non-commercial research.
•User may use extracts from the document in line with the concept of 'fair dealing' under the Copyright, Designs and Patents Act 1988 (?)
•Users may not further distribute the material nor use it for the purposes of commercial gain.

Where a licence is displayed above, please note the terms and conditions of the licence govern your use of this document.

When citing, please reference the published version.

Take down policy
While the University of Birmingham exercises care and attention in making items available there are rare occasions when an item has been uploaded in error or has been deemed to be commercially or otherwise sensitive.

If you believe that this is the case for this document, please contact UBIRA@lists.bham.ac.uk providing details and we will remove access to the work immediately and investigate.

Download date: 30. Apr. 2024

Current Biology

Macroevolutionary trends in theropod dinosaur feeding mechanics

--Manuscript Draft--

Manuscript Number:	CURRENT-BIOLOGY-D-21-00430R3
Full Title:	Macroevolutionary trends in theropod dinosaur feeding mechanics
Article Type:	Report
Corresponding Author:	Waisum Ma University of Birmingham Birmingham, West Midlands UNITED KINGDOM
First Author:	Waisum Ma
Order of Authors:	Waisum Ma
	Michael Pittman
	Richard J. Butler
	Stephan Lautenschlager
Abstract:	Theropod dinosaurs underwent some of the most remarkable dietary changes in vertebrate evolutionary history, shifting from ancestral carnivory1-3 to hypercarnivory4,5 and omnivory/herbivory6-9, with some taxa eventually reverting to carnivory10-12. The mandible is an important tool for food acquisition in vertebrates and reflects adaptations to feeding modes and diets13,14. The morphofunctional modifications accompanying the dietary changes in theropod dinosaurs are not well understood because most of the previous studies focused solely on the cranium and/or are phylogenetically limited in scope12,15-21, while studies that include multiple clades are usually based on linear measurements and/or discrete osteological characters8,22. Given the potential relationship between macroevolutionary change and ontogenetic pattern23, we also explore whether functional morphological patterns observed in theropod mandibular evolution show similarities to the ontogenetic trajectory. Here, we use finite element analysis to study the mandibles of non-avialan coelurosaurian theropods and demonstrate how feeding mechanics vary between dietary groups and major clades. We reveal an overall reduction in feeding-induced stresses along all theropod lineages through time. This is facilitated by a post-dentary expansion and the development of a downturned dentary in herbivores and an upturned dentary in carnivores likely via the “curved bone effect”. We also observed the same reduction in feeding-induced stress in ontogenetic series of jaws of the tyrannosaurids Tarbosaurus and Tyrannosaurus , which is best attributed to bone functional adaptation. This suggests that this common tendency for structural strengthening of the theropod mandible through time, irrespective of diet, is linked to ‘functional peramorphosis’ of bone functional adaptations acquired during ontogeny.
Additional Information:	
Question	**Response**
Standardized datasets A list of datatypes considered standardized under Cell Press policy is available here. Does this manuscript report new standardized datasets?	No
Original Code Does this manuscript report original code?	No

Powered by Editorial Manager® and ProduXion Manager® from Aries Systems Corporation

Click here to view linked References

Macroevolutionary trends in theropod dinosaur feeding mechanics

Waisum Ma[1,3,*], Michael Pittman[2], Richard J. Butler[1], Stephan Lautenschlager[1]

[1]School of Geography, Earth and Environmental Sciences, University of Birmingham, Birmingham, United Kingdom

[2]Vertebrate Palaeontology Laboratory, Research Division for Earth and Planetary Science, The University of Hong Kong, Hong Kong SAR, China

[3]Lead contact

*Correspondence: w.ma.1@pgr.bham.ac.uk

Twitter handle: @FionMaWS

Summary

Theropod dinosaurs underwent some of the most remarkable dietary changes in vertebrate evolutionary history, shifting from ancestral carnivory[1-3] to hypercarnivory[4,5] and omnivory/herbivory[6-9], with some taxa eventually reverting to carnivory[10-12]. The mandible is an important tool for food acquisition in vertebrates and reflects adaptations to feeding modes and diets[13,14]. The morphofunctional modifications accompanying the dietary changes in theropod dinosaurs are not well understood because most of the previous studies focused solely on the cranium and/or are phylogenetically limited in scope[12,15-21], while studies that include multiple clades are usually based on linear measurements and/or discrete osteological characters[8,22]. Given the potential relationship between macroevolutionary change and ontogenetic pattern[23], we also explore whether functional morphological patterns observed in theropod mandibular evolution show similarities to the ontogenetic trajectory. Here, we use finite element analysis to study the mandibles of non-avialan coelurosaurian theropods and demonstrate how feeding mechanics vary between dietary groups and major clades. We reveal an overall reduction in feeding-induced stresses along all theropod lineages through time. This is facilitated by a post-dentary expansion and the development of a downturned dentary in herbivores and an upturned dentary in carnivores likely via the "curved bone effect". We also observed the same reduction in feeding-induced stress in ontogenetic series of jaws of the tyrannosaurids *Tarbosaurus* and *Tyrannosaurus*, which is best attributed to bone functional adaptation. This suggests that this common tendency for structural strengthening of the theropod mandible through time, irrespective of diet, is linked to 'functional peramorphosis' of bone functional adaptations acquired during ontogeny.

Keywords: dinosaur, functional morphology, feeding mechanics, diet, skull, peramorphosis

Results

Mandibular stress distribution pattern

The feeding mechanics of 43 theropod taxa were visualised using FEA (Figures 1 and S1). When biting at the anterior tip, the mandibles of herbivores (Ornithomimosauria, Therizinosauria, Oviraptorosauria) are significantly more stress-resistant than those of the carnivores (Tyrannosauroidea, Dromaeosauridae), as demonstrated by von Mises stress plots (Figure 1) and average stress calculations (Figures. 2A-C; Table S1). This difference remains significant when taxa with exceptionally high mandibular stress, and allometric and phylogenetic signals are excluded (Table S1 & Data S1D). When carnivores bite at the last tooth, they experience reduced mandibular stress levels which are more similar to those of the anterior-biting herbivores (Figure 2A-C), although the difference remains significant when allometric and phylogenetic signals are removed (Table S1). Under all bite scenarios, the outgroup (comprising ancestral dinosaurs) differs significantly from herbivores in average stress, but not from carnivores (Table S1).

When compared to the outgroup, all five clades have a larger average stress resistance under both anterior- and posterior-bite scenarios (Figure 2B). The mandibles of tyrannosauroids are generally more stress-resistant than those of dromaeosaurids, although this difference is insignificant (Table S2). Oviraptorosaurians and ornithomimosaurians share similar mandibular robustness that is more stress-resistant than those of therizinosaurians in general under an anterior-bite scenario, but only the difference in the former pair is significant (Table S2). Within each of these five clades, a general trend of increasing mandibular stress resistance was identified along their respective lineages, as demonstrated by ancestral state reconstructions of empirical values and phylogenetic generalized least square regression (PGLS) residuals using linear parsimony and maximum likelihood (Figure S2A; Table S3; Data S1F-G). The observed mandibular stress under anterior-bite scenario is significantly smaller than the values simulated under Brownian motion evolution (before and after accounting for potential allometric and phylogenetic signals), confirming a trend of enhanced mandibular strength (Table S4), while that under posterior-bite scenario is significantly smaller before accounting for allometric and phylogenetic signals. Despite an overall increase in resistance, there are slight decreases in one of the later-diverging dromaeosaurid nodes (*Linheraptor* + *Tsaagan*) and some later-diverging oviraptorids, as well as a more substantial decrease in caenagnathid oviraptorosaurians later-diverging than *Gigantoraptor* (Figure S2).

Mature *Tyrannosaurus* and *Tarbosaurus* have mandibles that are more stress-resistant than their respective juvenile forms under both bite scenarios (Figure 3). This is also reflected in the reduction of stress/strain hotspots along ontogeny (Figure 3).

Bite efficiency and speed

In general, herbivores (Ornithomimosauria, Therizinosauria, Oviraptorosauria) have a significantly higher bite efficiency (defined as the percentage of input muscle force that is transferred into actual bite force) than carnivores (Tyrannosauroidea, Dromaeosauridae) when biting at the anterior tip (Figures 2D-F and Table S1). Consequently, the relative speed of jaw closure (i.e. inverse of bite efficiency) also shows a contrasting pattern in the carnivores and herbivores: carnivores, in general, have a higher jaw closing speed than herbivores. The disparity between herbivores and carnivores reduces when the bite point for carnivores is moved to the last tooth, achieving bite efficiency more similar to the herbivores (Figure 2D and Table S1). The outgroup exhibits a significant difference in bite efficiency when compared to carnivorous theropods but not to the herbivores (Table S1). Among all clades, oviraptorosaurians have the highest average bite efficiency under an anterior-bite scenario (Figure 2E). Under all bite scenarios, ornithomimosaurians have the lowest average bite efficiency (Figure 2E). Unexpectedly, a few extremely

downturned mandibles of herbivores (e.g. *Ornithomimus*, *Similicaudipteryx*, *Caudipteryx*) appear to have a bite efficiency under the anterior-bite scenario that is larger than or very similar to bite efficiency under the posterior-bite scenario (Figure 2F). The empirical data and PGLS residuals of posterior bite efficiency are significantly different from that simulated under Brownian motion evolution, while those of anterior bite efficiency do not show significant differences (Table S4).

The mandibles of mature *Tyrannosaurus* and *Tarbosaurus* allow them to bite faster than their respective juvenile forms under both anterior- & posterior- bite scenarios (Figure 3). However, they show a lower bite efficiency than the juveniles (Figure 3).

Simulated deformed mandible performance

FEA on the simulated deformed mandibles uncovered contrasting patterns between herbivorous (Ornithomimosauria, Therizinosauria, Oviraptorosauria) and carnivorous (Tyrannosauroidea, Dromaeosauridae) theropods (Figure 1). In most herbivores, deformed mandibles experience lower average stress than the original undeformed mandibles, whereas the pattern is reversed in carnivores (under both bite scenarios) (Data S1I & J). Almost all deformed mandibles attain a higher bite efficiency than those of the original mandibles under anterior bite scenarios (and consequently a reduced relative speed), but no obvious pattern is observed under posterior-bite scenarios.

Allometry and phylogeny

Phylogenetic generalized least square regression (PGLS) recovered significant correlations between mandibular length and average stress, but not between mandibular length and bite efficiency under all bite scenarios (Table S3).

Discussion

Diet-related difference in mandibular stress resistance, bite efficiency and relative bite speed

Herbivorous and carnivorous theropods exhibit different patterns in their feeding mechanics in terms of mandibular stress resistance, bite efficiency and relative bite speed. The difference between ancestral theropods and herbivores in average stress, and ancestral theropods and carnivores in bite efficiency demonstrate that the evolution of herbivory and more specialised carnivory has driven increased mandibular strength and decreased bite efficiency in the respective theropod lineages. This likely relates to the different functional demands for acquiring plants and meat respectively. When biting at the anterior tip, the mandibles of herbivorous theropods are more stress-resistant and bite-efficient than those of the carnivores, which facilitates repetitive cropping of fibrous and potentially tough plant parts. This corroborates the functional adaptions observed in extant herbivores which may also have a non-herbivorous ancestral diet. These adaptions include evolving a more stress-resistant mandible/skull[24,25], as well as a more efficient biting system in transferring input muscle forces into actual bite force[25-27]. Although these functional modifications could benefit predatory carnivores in general, speed is also an important factor determining hunting success. Given the inverse relationship between bite efficiency and relative bite speed, carnivores could not optimise the former indefinitely. The need to balance bite efficiency and speed likely explains why carnivorous theropod mandibles tend to be less bite efficient and

consequently less stress-resistant than those of herbivores (Figure 2). It is also noted that after accounting for allometric and phylogenetic signals, the difference in anterior bite efficiency between ancestral theropods and carnivores becomes insignificant (Table S1). This possibly suggests that the low bite efficiency in carnivores could be a by-product of selection for elongated snouts, a feature that facilitates active prey capture[24].

More similar mandibular stress resistance and bite efficiency patterns are detected in herbivorous and carnivorous theropods when the posterior-bite scenario for the carnivores is compared to the anterior-bite scenario for the herbivores (Figure 2). Herbivory and carnivory create different functional demands on animals, and so they are expected to show dissimilar mandibular mechanics under the same loading condition. However, when the corresponding, more realistic bite behaviours of herbivores and carnivores are simulated, such differences are reduced. This suggests that theropods tend to maintain similar levels of mandibular robustness and bite efficiency regardless of diet, which could be a result of bite position adjustment.

The jaw adduction system of theropod dinosaurs is a type III lever system. It is expected that the bite efficiency of a theropod mandible decreases as the bite position moves anteriorly. Surprisingly, we observe a very similar or even a larger bite efficiency (i.e. calculated using the vertical component of reaction force) at the anterior tip than that at the posteriormost bite position in extremely downturned mandibles (e.g. *Ornithomimus*, *Similicaudipteryx*, *Caudipteryx*; Figure 2F). This observation suggests that extreme mandibular morphology could influence the calculation of lever mechanics in the jaw adduction system of herbivorous theropods, due to the bite point of a downturned dentary being located substantially below the occlusal margin of the dentary. However, it is possible that the extreme downturned portion was covered with rhamphotheca in life, and that the overall shape of the lower jaw would have been less downturned. The simplification of muscle attachments and insertions involved may also be one of the factors leading to the observed result, which could be further tested with a more refined simulation in the future.

Simulated deformed mandibles uncover shared macroevolutionary trends and driver

We observed that the simulated deformed mandibles of early-diverging herbivorous theropods resemble those of the later-diverging members of their respective lineages under the anterior-bite scenario (e.g. *Jianchangosaurus*, *Segnosaurus*; Figure 1). Compared to the original mandible, the deformed mandibles usually possess a more downturned dentary and an elevated coronoid region (Figure 1). Among the mandibles of the herbivores, >75% of them show a decreased stress in the deformed mandibles (Data S1I & J), suggesting a higher stress resistance if the herbivores bite with the simulated deformed mandible instead of the corresponding original mandible. This is opposite to the pattern observed in most carnivorous theropods where the deformed mandible is less stress-resistant than the original one under all biting scenarios. Such differences in the stress resistance may explain why only the herbivores show a tendency of evolving mandibles that morphologically resemble those of the simulated deformed ones, as a more robust mandible is favoured by feeding specialisation.

Structural strengthening along lineages and feeding adaptations

Increased stress resistance is detected along all theropod lineages through time (Figure S2), suggesting selective pressure on mandibular robustness regardless of diet. Herbivores and carnivores achieved this

structural enhancement via different sets of modifications - they share similar morphological adaptions in the post-dentary region but contrasting patterns in the dentary. Dorsoventral expansion in the post-dentary region is a common stress-dissipation strategy employed by dinosaurs, including herbivorous and carnivorous theropods[28,29] and ornithischians[22]. This particularly strengthens the post-dentary region against dorsoventrally-directed forces, the major force vector experienced during jaw closure. This is important as the expansion also provides more space for adductor muscle attachment[30], which increases input muscle force by being able to accommodate larger muscle volumes.

While all theropods show expansion in the post-dentary region, herbivorous and carnivorous theropods evolved different morphologies in the dentary, which likely relates to the needs and limitations imposed by their respective feeding modes. Herbivorous mandibles with a more downturned dentary and a more dorsoventrally expanded post-dentary region display higher robustness than a straight, thin theropod mandible (Figure 1), as previously observed in therizinosaurians[28]. A downturned dentary has been considered a common adaption for herbivorous theropods[8,22] because of its stress-dissipating function[28]. The presence of a keratinous beak has been observed or inferred in non-avialan herbivorous theropods[8,18,21,31], and shown to have a further mandible stabilizing effect [18]. Together with a downturned dentary, these modifications allowed herbivorous theropods to exploit plant materials that were unavailable to earlier-diverging, non-herbivory-adapted theropods.

Despite the known biomechanical benefits of developing a downturned dentary, no tyrannosauroids and dromaeosaurids are known to have evolved ventrally deflected dentaries. This could relate to the fact that carnivores tend to have a 'scissor-like occlusal style'[32] due to the jaw joint being positioned at the same level as the tooth row, so the posterior teeth tend to be used more frequently for food acquisition. At the same time, tooth positions closer to the jaw joint have the highest mechanical advantage. As shown in the von Mises stress plots under the posterior-bite scenario (Figure S1), the stress experienced by the dentary is minimal. Thus, there is smaller evolutionary pressure for the carnivores to strengthen the anterior part of their mandible relative to the herbivores. Another reason for the lack of a downturned dentary in tyrannosauroids and dromaeosaurids might be, most importantly, the limitation on mandibular morphology imposed by predation. For carnivores that perform regular hunting, having a downturned dentary may not be favourable for prey anchorage. Compared to the earliest carnivorous theropods, later-diverging tyrannosauroids and dromaeosaurids evolved an upturned dentary with an undulating occlusal margin resembling that of the carnivorous spinosaurid theropods[33] and modern predators like crocodiles[34]. Such a mandibular morphology likely allowed them to anchor prey tightly, facilitating hunting.

Although carnivorous theropods did not evolve a stress-dissipating downturned dentary, we suspect that their upturned dentary, apart from facilitating prey anchorage, could reduce feeding-induced stress through a 'curved bone effect'. Many long bones of vertebrates are curved, but whether such morphology is mechanically beneficial has been controversial[35-37], as it was suggested that a curved bone is weakened compared to a straight bone[35,38]. Recent finite element analyses of extant mammalian long bones demonstrate that such curvature is likely an adaptation to counter the stress/strain induced by habitual loading[36,37,39]. Although located in different body parts, the deformation simulation in our study demonstrates a similar mechanical response in theropod mandibles: when a theropod with an upturned mandible bites, the mandible bends downward and tends to become straightened (Figure 1). It also shows that a curved mandible (e.g. original mandible of *Tyrannosaurus rex*) is more stress-resistant than the straightened equivalent (e.g. simulated deformed mandible of *Tyrannosaurus rex*) (Data S1I & J). We hypothesise that the mandibles of later-diverging tyrannosauroids and dromaeosaurids could have benefited from the 'curved bone effect', where the upturned dentary acts as a pre-bent structure and dissipates stress/strain when it deforms under habitual feeding load.

Bone functional adaptation and evolutionary pattern

We suspect that the evolutionary trends of theropod mandible function share a similar trajectory with ontogenetic changes inferred from bone functional adaptation principles. When an animal bites, areas of high stress and strain under such habitual loading will be remodeled to increase mandibular strength[40]. Common strategies of bone-strengthening include the addition of bone mass and alteration of bone geometry and microstructure[41]. Based on bone functional adaptation, we could plausibly hypothesise that bone-strengthening will happen in these high strained regions as the individual develops (assuming growth is still in progress), so as to increase the mandible's adaptiveness to biting-induced loading. If we apply the same loading to the 'remodeled mandible', one could expect it to show higher resistance than the 'less-remodeled mandible'. Our results show that the mandibles of *Tyrannosaurus* and *Tarbosaurus* become more resistant to biting-induced stress as they develop from juvenile to adult (Figure 3), suggesting overall mechanical strengthening. A study of tyrannosaurid mandibles recovered a similar trend of ontogenetic structural strengthening based on beam modelling[42] as well as 2D and 3D FEA[43]. However, the extent to which bone functional adaptation is responsible for such changes in mandibular biomechanics requires further investigation. Bone functional adaptation in non-avialan dinosaurs has rarely been commented on, except for taxa that are known from ontogenetic series: the cranium of *Tyrannosaurus* does not show a close association between high strained regions and regions that have undergone the most morphological changes during ontogeny, which was interpreted as a lack of bone remodelling[44]. However, it is also possible that such a relationship is not applicable to the mandible, as the theropod cranium serves wider roles than the mandible and these roles may impose constraints on cranial morphology[45,46]. Although the mechanism is currently unclear, we suspect that bone functional adaptation could have played a part in the ontogenetic mechanical strengthening pattern observed in non-avialan theropod mandibles.

Interestingly, similar trends of mechanical strengthening are observed in theropod mandible evolution as demonstrated by increased stress resistance (Figure S2A; Table S3) and reduction of stress/strain hotspots along all lineages (Figure 1 & S1). As discussed above, such strengthening is likely to be achieved through dorsoventral expansion of the post-dentary region (for all lineages) and a downturned dentary (for herbivorous lineages) or an upturned dentary (for carnivorous lineages): the extent of these modifications is observed to be more prominent in later-diverging members of the lineages (Figure 1)[47-49]. Our results, therefore, show that the mandibular function of non-avialan theropods changes with a similar trajectory across ontogeny and phylogeny, demonstrating a pattern of "functional peramorphosis" (Figure 4). Several morphological traits in non-avialan dinosaurs are known to be paedomorphic or peramorphic[50-53]. However, the functional significance of these traits has not been quantified and thus their evolutionary trends remain unclear, given bone morphology and function may not be tightly linked[54]. This study represents an initial attempt to quantify a heterochronic pattern from a functional perspective, which demonstrates how "functional peramorphosis" could have facilitated the mandibular evolution of non-avialan theropods.

Intra-clade variations in feeding mechanics and diets

Although theropod clades can be broadly classified into carnivory and herbivory, it is well-noted that feeding mechanics and diets could vary between and within each clade. For example, dromaeosaurids and tyrannosauroids are both considered hypercarnivores[55], but their body size variations imply their diets presumably differed through the targeting of prey of different sizes[56]. In fact, their niche differences

are partially reflected in our analysis: dromaeosaurids have mandibles that are generally less robust but allow them to bite faster compared to those of tyrannosauroids (Figure 2). Although herbivorous theropods are generally more bite efficient than carnivores, our results show that ornithomimosaurs have the lowest average bite efficiency among all study clades (Figure 2E). This highlights that certain aspects of the feeding strategies of herbivorous theropods are variable to an extent that overlap with those of carnivores. Dietary reversals to omnivory/carnivory are suspected in the ornithomimosaurian *Deinocheirus* and later-diverging caenagnathid oviraptorosaurians[10-12] based on direct and anatomical/functional evidence respectively. Our results add to these studies by showing that later-diverging caenagnathids have some of the most speed-efficient mandibles among oviraptorosaurians (Figure S2), which could have been an adaptation for prey capture. As in carnivorous theropods[57], body size might also be a factor affecting feeding mechanics: exceptionally large herbivorous theropods like *Deinocheirus* and *Gigantoraptor* display stress/strain distribution patterns that are unlike other members in the same clade (Figures 1 & S1), which supports hypotheses that they were specialised feeders[10,21,58]. The presence of large-bodied members in every herbivorous theropod clade[9] suggests that size-related niche partitioning might have been widespread among them. Such ecological niche partitioning could have contributed to the diversification of theropod dinosaurs, which eventually led to the rise of modern birds.

Acknowledgements

We would like to thank the Institute of Vertebrate Paleontology and Paleoanthropology, Henan Geological Museum, Dongyang Museum and Shandong Tianyu Museum of Nature for access to specimens in their care. W.M. was supported by Richard Osgood Student Research Award from the Paleontological Society and funds from The University of Hong Kong (HKU) MOOC Dinosaur Ecosystems. M.P.'s participation in this study was funded by the Research Grant Council General Research Fund (17103315, 17120920 and 17105221), RAE Improvement Fund of the Faculty of Science, HKU and the HKU MOOC Dinosaur Ecosystems.

Author Contributions

W.M. and S.L. conceived the project. W.M. carried out the experiments. W.M. and S.L. analysed the data. W.M. wrote the first draft of the manuscript. All authors wrote and revised the final manuscript. All authors approved the manuscript for publication.

Declaration of Interests

The authors declare no competing interests.

Figure legends

Figure 1. Comparison of von Mises stress plots of non-avialan theropod mandibles under an anterior-bite scenario. Left: original mandible; Right: simulated deformed mandible, showing the deformation (displacement) of the original mandible under loading and the biomechanical performance of this simulated form (see methods). Silhouettes modified from PhyloPic. See also Figures S1-3,

Figure 2. Biomechanical performance of the original mandibles of the non-avialan theropods studied under anterior-bite and posterior-bite scenarios. Average mandibular stress of (**A**) major clades; (**B**) dietary groups; (**C**) theropod taxa. Bite efficiency of (**D**) major clades; (**E**) dietary groups; (**F**) theropod taxa. See Figure 2B for legend. p < 0.001=***, < 0.01=**, < 0.05=*. Silhouettes modified from PhyloPic. See also Figures S2-3 and Tables S1-2.

Figure 3. Comparison of biomechanical performance of the tyrannosauroids *Tyrannosaurus* and *Tarbosaurus*, demonstrating structural strengthening and increase in relative jaw-closing speed through ontogeny. (**A**) Average mandibular stress. (**B**) Bite efficiency.

Figure 4. 'Functional peramorphosis' of bone functional adaptation in the mandibles of non-avialan theropods. Schematic diagram summarising the functional morphological adaptations and structural strengthening observed in theropod mandibles accompanying dietary specialisations, using Tyrannosauroidea and Therizinosauria as examples. Silhouettes modified from PhyloPic.

STAR Methods

Resource availability

Lead contact

Further information and requests for resources should be directed to the lead contact, Waisum Ma (w.ma.1@pgr.bham.ac.uk).

Materials availability

This study did not generate new reagents.

Data and code availability

The datasets of this study are available with the manuscript and deposited on the public repository Zenodo: https://doi.org/10.5281/zenodo.5654785. Any additional information is available from the lead contact upon request.

Experimental model and subject details

Experimental models are theropod dinosaur fossils accessioned at public institutions where the specimens are available for research. See Data S1A for additional information.

Specimens

For this study, 45 non-avialan theropod mandibles were analysed (Data S1A) comprising 43 species (including two juvenile-adult pairs) from five coelurosaurian clades: Tyrannosauroidea, Ornithomimosauria, Therizinosauria, Oviraptorosauria and Dromaeosauridae. Three early-diverging dinosaurs were also analysed as outgroup taxa (*Herrerasaurus*, *Eoraptor*, *Tawa*), noting that *Herrerasaurus* and *Tawa* were suggested to be carnivores and *Eoraptor* to be an omnivore/herbivore

based on anatomical features[1,2]. The tyrannosauroids *Tyrannosaurus rex* and *Tarbosaurus bataar* were chosen for ontogenetic comparison as only these theropod species preserve complete mandibles with age estimations based on histological analysis[44,50,51]. The five clades are classified into two dietary groups—carnivory (Tyrannosauroidea, Dromaeosauridae) and herbivory (Ornithomimosauria, Therizinosauria, Oviraptorosauria)—based on previous inferences encompassing extrinsic, anatomical, statistical and biomechanical evidence[5-8,17]. We recognise that some species within these clades may not conform to this broad classification due to potential dietary reversal[10-12]. These exceptional cases are discussed in more detail in the main text.

Method details

Model generation

Simplified, extruded models[62] were generated based on the lateral profiles of theropod mandibles. Photographs were taken first-hand in museum collections where possible, while the remaining photographs/figures were obtained from published literature (Data S1A). Only specimens that are well-preserved or have undergone a low degree of deformation and breakage were included in the study. Reconstructions of specimens were obtained from the corresponding published literature where provided. The extruded models were created in the 3D animation software *Blender* (version 2.79b, www.blender.org). All extruded models were scaled to the same anteroposterior length, with a consistent thickness of 2% of the length. The element size is 2.2×10^{-4} for all models. The total number of elements per model is available in Data S1B. We recognize that the mandibular thickness of theropods is unlikely to be homogeneous, and that certain mandibular portions of some theropods (e.g. oviraptorosaurians) are deflected medially. Although the models cannot replicate every aspect of mandibular morphology, the approach used herein allows the comparison of feeding mechanics at a broad scale, particularly the dorsoventral bending component of biting.

Finite element analysis

Finite element analysis (FEA) was conducted for all models (see Figure S4 for the workflow). Extruded 2D finite element models can be as informative as 3D models under a comparative context[62], and this approach has been widely used in biological and medical research[63-69]. A study involving various tyrannosaurid mandibles validated the use of extruded 2D finite element models in comparing theropod mandibular strength, via a comprehensive comparison with the results from 3D FEA[43]. Given the time constraints and logistical difficulties in collecting 3D data for all taxa, extruded models are particularly suitable for large-scale analyses that incorporate a substantial number of specimens. Such simplified models are also advantageous because they can incorporate fossil specimens preserved within slabs (rather than in 3D), a common form of preservation for the early-diverging members of many major non-avian theropod clades[70].

Pre-FEA model setup was performed in *Hypermesh* (version 11, Altair Engineering Inc.). The material property of the models ($E = 20.49$ GPa, $\upsilon = 0.4$) was taken from an alligator mandible, an extant analogue of non-avian dinosaurs[71], as implemented in previous FEA studies on theropods[18,28]. To compare the feeding mechanics of the mandibles, we set up two loading conditions that resemble bite action. The anterior-biting scenario places the bite position at the first tooth for a toothed mandible, or at the most anterior tip for a toothless mandible. The posterior bite scenario places the bite location at the last tooth

or at the posterior-most point of the inferred rhamphotheca[18,19,21]. This latter scenario takes into account the more realistic feeding mode of carnivores, which usually process food using more posterior teeth[72,73]. For both scenarios, eight muscles were reconstructed for each mandibular model, with reference to previous jaw muscle reconstructions[17,19-21,30] (see Data S1C for details of muscle attachment sites and insertion angles). Muscle forces implemented on each model were standardised (i.e. 80 N in total for each model) as for the length of the models[43,74]. All models were constrained at the jaw joint from x-, y- and z-direction movement.

After setting up the material properties and loading conditions, the models were imported into *Abaqus* (version 6.141, Dassault Systèmes Simulia Corp.) for analysis. Stress and strain distribution of the mandibles under the bite scenarios were visualised as von Mises stress diagrams and the average stress of each model was calculated. The von Mises stress was used for comparison as it predicts how close a structure will yield or fracture, such that a lower stress value indicates a higher strength. Appropriate stress limits were used in the diagrams to provide a consistent maximum resolution of the contour plots across all studied taxa, accommodating both low- and high-stress regimes well. Bite efficiency was also calculated for each model, defined as the percentage of input muscle force that is transferred into actual bite force. The node value of the vertical component of the reaction force at the bite location was measured for bite force efficiency calculation. Given the known inverse relationship between mechanical advantage (i.e. bite efficiency) and speed, the relative bite speed of the mandibles was calculated as the inverse of the bite efficiency.

Ancestral state reconstructions using linear parsimony and maximum likelihood were conducted in *Mesquite* (version 3.61[59]) and R package phytools (version 0.7-70[75]) (R version 4.1.1[61]) respectively to track the change of biomechanical characters across the evolutionary tree. The phylogeny used in this study is a time-scaled composite of several simplified strict consensus trees (see Supplementary Figure 20 for details). Time-scaling was conducted in R using the “equal” method of the function DatePhylo in the R package strap (version 1.4[76]) (R version 3.4.4[61]). Analysis of variance (ANOVA) was conducted to compare the biomechanical differences between carnivorous and herbivorous non-avialan theropods. Additional ANOVA was conducted excluding taxa that have an exceptionally high average mandibular stress (i.e. *Tawa* & *Buitreraptor*), in order to investigate their potential influence on intergroup comparisons. Statistical analyses were performed in the software *PAST* (version 3.18[60]). We also compared the observed evolutionary trends with the values simulated under Brownian motion using the function ‘fastBM’ in the R package phytools (version 0.7-70[75]), with the range of the simulated values following the maximum and minimum values in the corresponding empirical dataset. The ancestral state at the root node was taken from the results of maximum likelihood ancestral state reconstruction. We tested whether the simulated values are significantly different from the empirical values by conducting a bootstrap Kolmogorov-Smirnov using the function ‘ks.boot’ in R package Matching (version 4.9-5[77]).

Finite element analysis of simulated deformed mandibles

When the mandibles are subjected to feeding-induced forces, deformation occurs. With FEA, the ‘deformed morphology’ of the mandibles can be visualised to show the direction and extent of deformation (displacement) under feeding scenarios. Although the deformation has been exaggerated by a given factor, we were interested in generating simulated deformed mandibles and investigating their biomechanics under the deformed state. By comparing them with that of the original mandibles, we identified any possible changes in biomechanics, and whether such changes differ between dietary groups. The deformed morphologies of the mandibles were visualised in *Abaqus* using auto-compute

scaling. The lateral profiles of the deformed mandibles were captured in *Abaqus*. The outline of each lateral profile was traced to produce a 2D model in *Blender* (version 2.79b, www.blender.org) under the same procedure implemented for the original mandibles. Pre-FEA setup and FEA were also conducted following the above protocols.

Allometry and phylogeny

To test the potential effect of allometry on mandibular biomechanics, we conducted phylogenetic generalized least square regression (PGLS) between biomechanical characters and mandibular length. The analysis was conducted using the R packages ape (version 5.1[78]), nlme (version 3.1.131[79]) and geiger (version 2.0.6[80]). The residuals of PGLS were subjected to ancestral state reconstructions and comparison with Brownian motion simulated values following the protocol outlined above, allowing us to study the trend after accounting for the potential allometric and phylogenetic signals.

Quantification and statistical analysis

All statistical analyses were performed in the software *PAST* (version 3.18[60]) and R (version 4.1.1[61]). P-values < 0.05 were considered significant (p < 0.001=***, < 0.01=**, < 0.05=*). Analysis of variance (ANOVA) was used to compare the biomechanical differences between groups of non-avialan theropods. Bootstrap Kolmogorov-Smirnov test was conducted to test the differences between empirical values of biomechanical characters and values simulated under Brownian motion. Phylogenetic generalized least square regression (PGLS) was performed to test for allometric signal in the biomechanical dataset.

Data S1. Tables associated with biomechanical and statistical analyses, related to STAR Methods and Figures 1-3. (A) List of taxon and specimens included in the study. (B) Number of tetrahedral elements of finite element models. (C) Muscle attachments for non-avialan theropods used in this study. For each clade, a representative (which preserves a complete skull and/or its skull myology has been studied previously) is chosen for inferring muscle attachment locations and angles for the respective clade. Missing cranial portions are estimated based on closely related taxa or published reconstructions. (D) Differences in mandibular biomechanics between dietary groups of Theropoda shown by Analysis of Variance (ANOVA), excluding *Tawa* and *Buitreraptor*. Results conducted using the residuals of conducted phylogenetic generalized least square regression (PGLS) are in brackets. (E) Differences in mandibular biomechanics between theropod clades by Analysis of Variance (ANOVA), excluding *Tawa* and *Buitreraptor*. Results conducted using the residuals of conducted phylogenetic generalized least square regression (PGLS) are in brackets. (F) Reconstructed ancestral states of biomechanical characters using maximum likelihood. Node comprising all the taxa of the corresponding clade is in red. (G) Reconstructed ancestral states of the residuals of biomechanical characters using maximum likelihood. Node comprising all the taxa of the corresponding clade is in red. (H) First and last appearance dates of the studied taxa. (I) Biomechanical performance of the original mandibles. (J) Biomechanical performance of the simulated deformed mandibles. (K) Supplemental references.

References

1 Nesbitt, S. J. *et al.* A complete skeleton of a Late Triassic saurischian and the early evolution of dinosaurs. *Science* **326**, 1530-1533 (2009).
2 Martinez, R. N. *et al.* A basal dinosaur from the dawn of the dinosaur era in southwestern Pangaea. *Science* **331**, 206-210 (2011).
3 Müller, R. T. & Garcia, M. S. A paraphyletic 'Silesauridae' as an alternative hypothesis for the initial radiation of ornithischian dinosaurs. *Biology Letters* **16**, 20200417 (2020).
4 Norell, M. A. & Makovicky, P. J. in *The Dinosauria* (eds D.B. Weishampel, P. Dodson, & H. Osmólska) 196-209 (University of California Press, 2004).
5 Brusatte, S. L. *et al.* Tyrannosaur paleobiology: new research on ancient exemplar organisms. *Science* **329**, 1481-1485 (2010).
6 Ji, Q., Currie, P. J., Norell, M. A. & Ji, S. A. Two feathered dinosaurs from northeastern China. *Nature* **393**, 753-761 (1998).
7 Kobayashi, Y. *et al.* Herbivorous diet in an ornithomimid dinosaur. *Nature* **402**, 480-481 (1999).
8 Zanno, L. E. & Makovicky, P. J. Herbivorous ecomorphology and specialization patterns in theropod dinosaur evolution. *Proceedings of the National Academy of Sciences* **108** (2011).
9 Zanno, L. E. & Makovicky, P. J. No evidence for directional evolution of body mass in herbivorous theropod dinosaurs. *Proceedings of the Royal Society of London B: Biological Sciences* **280**, 20122526 (2013).
10 Lee, Y.-N. *et al.* Resolving the long-standing enigmas of a giant ornithomimosaur *Deinocheirus mirificus*. *Nature* **515**, 257-260 (2014).
11 Funston, G. F., Currie, P. J. & Burns, M. E. New elmisaurine specimens from North America and their relationship to the Mongolian *Elmisaurus rarus*. *Acta Palaeontologica Polonica* **61**, 159-173 (2015).
12 Ma, W., Pittman, M., Lautenschlager, S., Meade, L. E. & Xu, X. in *Pennaraptoran theropod dinosaurs: past progress and new frontiers* Vol. 440 (eds Michael Pittman & Xing Xu) Ch. 8, 229-250 (Bulletin of the American Museum of Natural History, 2020).
13 Olson, E. C. Jaw mechanisms: rhipidistians, amphibians, reptiles. *American Zoologist*, 205-215 (1961).
14 Hiiemae, K. M. Feeding in mammals. *Feeding: Form, function, and evolution in tetrapod vertebrates* **1**, 411-448 (2000).
15 Sakamoto, M. Jaw biomechanics and the evolution of biting performance in theropod dinosaurs. *Proceedings of the Royal Society B: Biological Sciences* **277**, 3327-3333 (2010).
16 Brusatte, S. L., Sakamoto, M., Montanari, S., Harcourt, S. & William, E. H. The evolution of cranial form and function in theropod dinosaurs: insights from geometric morphometrics. *Journal of Evolutionary Biology* **25**, 365-377 (2012).
17 Lautenschlager, S. Cranial myology and bite force performance of *Erlikosaurus andrewsi*: a novel approach for digital muscle reconstructions. *Journal of Anatomy* **222**, 260-272 (2013).
18 Lautenschlager, S., Witmer, L. M., Altangerel, P. & Rayfield, E. J. Edentulism, beaks, and biomechanical innovations in the evolution of theropod dinosaurs. *Proceedings of the National Academy of Sciences* **110** (2013).
19 Cuff, A. R. & Rayfield, E. J. Retrodeformation and muscular reconstruction of ornithomimosaurian dinosaur crania. *PeerJ* **3**, e1093 (2015).
20 Lautenschlager, S. Estimating cranial musculoskeletal constraints in theropod dinosaurs. *Royal Society Open Science* **2**, 150495 (2015).
21 Ma, W. *et al.* Functional anatomy of a giant toothless mandible from a bird-like dinosaur: *Gigantoraptor* and the evolution of the oviraptorosaurian jaw. *Scientific Reports* **7**, 16247 (2017).
22 Button, D. J. & Zanno, L. E. Repeated evolution of divergent modes of herbivory in non-avian dinosaurs. *Current Biology* **30**, 158-168. e154 (2020).
23 Gould, S. J. *Ontogeny and phylogeny*. (Harvard University Press, 1977).

24 Metzger, K. A. & Herrel, A. Correlations between lizard cranial shape and diet: a quantitative, phylogenetically informed analysis. *Biological Journal of the Linnean Society* **86**, 433-466 (2005).
25 Samuels, J. X. Cranial morphology and dietary habits of rodents. *Zoological Journal of the Linnean Society* **156**, 864-888 (2009).
26 Stayton, C. T. Testing hypotheses of convergence with multivariate data: morphological and functional convergence among herbivorous lizards. *Evolution* **60**, 824-841 (2006).
27 Navalón, G., Bright, J. A., Marugán-Lobón, J. & Rayfield, E. J. The evolutionary relationship among beak shape, mechanical advantage, and feeding ecology in modern birds. *Evolution* **73**, 422-435 (2018).
28 Lautenschlager, S. Functional niche partitioning in Therizinosauria provides new insights into the evolution of theropod herbivory. *Palaeontology* **60**, 375-387 (2017).
29 Schaeffer, J., Benton, M. J., Rayfield, E. J. & Stubbs, T. L. Morphological disparity in theropod jaws: comparing discrete characters and geometric morphometrics. *Palaeontology* (2019).
30 Holliday, C. M. New insights into dinosaur jaw muscle anatomy. *The Anatomical Record* **292**, 1246-1265 (2009).
31 Norell, M. A., Makovicky, P. J. & Currie, P. J. The beaks of ostrich dinosaurs. *Nature* **412**, 873-874 (2001).
32 Greaves, W. Functional implications of mammalian jaw joint position. *Forma et functio* **7**, 363-376 (1974).
33 Sasso, C. D., Maganuco, S., Buffetaut, E. & Mendez, M. A. New information on the skull of the enigmatic theropod *Spinosaurus*, with remarks on its size and affinities. *Journal of Vertebrate Paleontology* **25**, 888-896 (2005).
34 Cleuren, J. & De Vree, F. Feeding in crocodilians. *Feeding: form, function, and evolution in tetrapod vertebrates*, 337-358 (2000).
35 Jade, S., Tamvada, K. H., Strait, D. S. & Grosse, I. R. Finite element analysis of a femur to deconstruct the paradox of bone curvature. *Journal of Theoretical Biology* **341**, 53-63 (2014).
36 Milne, N. Curved bones: an adaptation to habitual loading. *Journal of Theoretical Biology* **407**, 18-24 (2016).
37 McCabe, K., Henderson, K., Pantinople, J., Richards, H. L. & Milne, N. Curvature reduces bending strains in the quokka femur. *PeerJ* **5**, e3100 (2017).
38 Bertram, J. E. & Biewener, A. A. Bone curvature: sacrificing strength for load predictability? *Journal of Theoretical Biology* **131**, 75-92 (1988).
39 Henderson, K., Pantinople, J., McCabe, K., Richards, H. L. & Milne, N. Forelimb bone curvature in terrestrial and arboreal mammals. *PeerJ* **5**, e3229 (2017).
40 Inou, N., Iioka, Y., Fujiwara, H. & Maki, K. in *Computational Biomechanics* 23-42 (Springer, 1996).
41 Pearson, O. M. & Lieberman, D. E. The aging of Wolff's "law": ontogeny and responses to mechanical loading in cortical bone. *American Journal of Physical Anthropology* **125**, 63-99 (2004).
42 Therrien, F., Henderson, D. M. & Ruff, C. B. in *The Carnivorous Dinosaurs* (ed Kenneth Carpenter) 179-237 (Indiana University Press, 2005).
43 Rowe, A. J. & Snively, E. Biomechanics of juvenile tyrannosaurid mandibles and their implications for bite force: Evolutionary biology. *The Anatomical Record* (2021).
44 Carr, T. D. A high-resolution growth series of *Tyrannosaurus rex* obtained from multiple lines of evidence. *PeerJ* **8**, e9192 (2020).
45 Witmer, L. M. Nostril position in dinosaurs and other vertebrates and its significance for nasal function. *Science* **293**, 850-853 (2001).
46 Lü, J. *et al.* High diversity of the Ganzhou Oviraptorid Fauna increased by a new "cassowary-like" crested species. *Scientific Reports* **7**, 6393 (2017).

47 Holtz, T. in *The Dinosauria* (eds D. B. Weishampel, H Osmólska, & P Dodson) Ch. 111-136, (University of California Press, 2004).
48 Pu, H. *et al.* An unusual basal therizinosaur dinosaur with an ornithischian dental arrangement from Northeastern China. *PloS one* **8** (2013).
49 Zanno, L. E., Tsogtbaatar, K., Chinzorig, T. & Gates, T. A. Specializations of the mandibular anatomy and dentition of *Segnosaurus galbinensis* (Theropoda: Therizinosauria). *PeerJ* **4**, e1885 (2016).
50 Plateau, O. & Foth, C. Birds have peramorphic skulls, too: anatomical network analyses reveal oppositional heterochronies in avian skull evolution. *Communications Biology* **3**, 1-12 (2020).
51 Bhullar, B.-A. S. *et al.* Birds have paedomorphic dinosaur skulls. *Nature* **487**, 223-226 (2012).
52 McNamara, K. J. & Long, J. A. in *The Complete Dinosaur. Life of the Past* 761-784 (Indiana University Press, 2012).
53 Wang, S. *et al.* Heterochronic truncation of odontogenesis in theropod dinosaurs provides insight into the macroevolution of avian beaks. *Proceedings of the National Academy of Sciences* **114**, 10930-10935 (2017).
54 Lautenschlager, S., Brassey, C. A., Button, D. J. & Barrett, P. M. Decoupled form and function in disparate herbivorous dinosaur clades. *Scientific reports* **6**, 26495 (2016).
55 Fastovsky, D. E. & Smith, J. B. in *The Dinosauria* (eds David. B. Weishampel, Peter Dodson, & Halszka Osmolska) Ch. 26, 614-626 (University of California Press, 2004).
56 Van Valkenburgh, B. & Molnar, R. E. Dinosaurian and mammalian predators compared. *Paleobiology* **28**, 527-543 (2002).
57 Therrien, F., Zelenitsky, D. K., Voris, J. T. & Tanaka, K. Mandibular force profiles and tooth morphology in growth series of *Albertosaurus sarcophagus* and *Gorgosaurus libratus* (Tyrannosauridae: Albertosaurinae) provide evidence for an ontogenetic dietary shift in tyrannosaurids. *Canadian Journal of Earth Sciences* (2021).
58 Ma, W., Brusatte, S. L., Lü, J. & Sakamoto, M. The skull evolution of oviraptorosaurian dinosaurs: the role of niche partitioning in diversification. *Journal of Evolutionary Biology* **33**, 178-188 (2020).
59 Maddison, W. P. & Maddison, D. R. Mesquite: a modular system for evolutionary analysis. *Evolution* **62**, 1103-1118 (2008).
60 Hammer, Ø., Harper, D. & Ryan, P. PAST: Paleontological Statistics software package for education and data analysis. *Palaeontologia Electronica* **4**, 1-9 (2001).
61 R Development Core Team. R: A language and environment for statistical computing. (2013).
62 Morales-García, N. M., Burgess, T. D., Hill, J. J., Gill, P. G. & Rayfield, E. J. The use of extruded finite-element models as a novel alternative to tomography-based models: a case study using early mammal jaws. *Journal of the Royal Society Interface* **16**, 20190674 (2019).
63 Dejak, B., Młotkowski, A. & Romanowicz, M. Finite element analysis of stresses in molars during clenching and mastication. *The Journal of Prosthetic Dentistry* **90**, 591-597 (2003).
64 Neenan, J. M., Ruta, M., Clack, J. A. & Rayfield, E. J. Feeding biomechanics in Acanthostega and across the fish–tetrapod transition. *Proceedings of the Royal Society B: Biological Sciences* **281**, 20132689 (2014).
65 Serrano-Fochs, S., De Esteban-Trivigno, S., Marcé-Nogué, J., Fortuny, J. & Fariña, R. A. Finite element analysis of the cingulata jaw: an ecomorphological approach to armadillo's diets. *PLoS One* **10**, e0120653 (2015).
66 Lautenschlager, S., Figueirido, B., Cashmore, D. D., Bendel, E.-M. & Stubbs, T. L. Morphological convergence obscures functional diversity in sabre-toothed carnivores. *Proceedings of the Royal Society B: Biological Sciences* **287**, 20201818 (2020).
67 Miller, C. V. *et al.* Disassociated rhamphotheca of fossil bird *Confuciusornis* informs early beak reconstruction, stress regime, and developmental patterns. *Communications Biology* **3**, 1-6 (2020).

68 Snively, E., Anderson, P. S. & Ryan, M. J. Functional and ontogenetic implications of bite stress in arthrodire placoderms. *Kirtlandia* **57**, 53-60 (2010).
69 Rayfield, E. J. Structural performance of tetanuran theropod skulls, with emphasis on the Megalosauridae, Spinosauridae and Carcharodontosauridae. *Special Papers in Palaeontology* **86**, 241-253 (2011).
70 Benton, M. J., Zhonghe, Z., Orr, P. J., Fucheng, Z. & Kearns, S. L. The remarkable fossils from the Early Cretaceous Jehol Biota of China and how they have changed our knowledge of Mesozoic life. *Proceedings of the Geologists' Association* **119**, 209-228 (2008).
71 Zapata, U. *et al.* Material properties of mandibular cortical bone in the American alligator, Alligator mississippiensis. *Bone* **46**, 860-867 (2010).
72 Greaves, W. S. Functional predictions from theoretical models of the skull and jaws in reptiles and mammals. *Functional morphology in Vertebrate Paleontology*, 99-115 (1995).
73 Erickson, G. M. *et al.* Bite-force estimation for *Tyrannosaurus rex* from tooth-marked bones. *Nature* **382**, 706-708 (1996).
74 Marcé Nogué, J., DeMiguel, D., Fortuny Terricabras, J., Esteban Trivigno, S. d. & Gil Espert, L. Quasi-homothetic transformation for comparing the mechanical performance of planar models in biological research. *Palaeontologia electronica* **16**, 1-15 (2013).
75 Revell, L. J. phytools: an R package for phylogenetic comparative biology (and other things). *Methods in ecology and evolution* **3**, 217-223 (2012).
76 Bell, M. A. & Lloyd, G. T. strap: an R package for plotting phylogenies against stratigraphy and assessing their stratigraphic congruence. *Palaeontology* **58**, 379-389 (2015).
77 Sekhon, J. S. Multivariate and propensity score matching software with automated balance optimization: the matching package for R. *Journal of Statistical Software, Forthcoming* (2008).
78 Paradis, E. & Schliep, K. ape 5.0: an environment for modern phylogenetics and evolutionary analyses in R. *Bioinformatics* **35**, 526-528 (2019).
79 Pinheiro, J. nlme: linear and nonlinear mixed effects models. R package version 3.1-98. *https://cran.r-project.org/web/packages/nlme/* (2011).
80 Harmon, L. J., Weir, J. T., Brock, C. D., Glor, R. E. & Challenger, W. GEIGER: investigating evolutionary radiations. *Bioinformatics* **24**, 129-131 (2008).

Key resources table

REAGENT or RESOURCE	SOURCE	IDENTIFIER
Deposited data		
Finite element analysis: model parameters and von Mises stress and maximum principal strain plots	This paper	Data S1; https://doi.org/10.5281/zenodo.5654785
Ancestral state reconstruction using linear parsimony and maximum likelihood	This paper	Data S1; https://doi.org/10.5281/zenodo.5654785
Biomechanical performance of mandibles	This paper	Data S1; https://doi.org/10.5281/zenodo.5654785
Phylogeny used in this study	This paper	Data S1; https://doi.org/10.5281/zenodo.5654785
Software and algorithms		
Abaqus 6.141	Dassault Systèmes Simulia Corp.	www.3ds.com/products-services/simulia/products/abaqus/
Avizo 9.1	Thermo Fisher Scientific	www.thermofisher.com/hk/en/home/electron-microscopy/products/software-em-3d-vis/avizo-software.html
Blender 2.79b	Blender Foundation	www.blender.org
Hypermesh 11	Altair Engineering Inc.	www.altair.com/hypermesh
Mesquite 3.61	[59]	www.mesquiteproject.org
PAST 3.18	[60]	http://priede.bf.lu.lv/ftp/pub/TIS/datu_analiize/PAST/2.17c/download.html
R 4.1.1	[61]	https://cran.r-project.org

Figure 3

Click here to access/download;Figure;CB_fig3.png

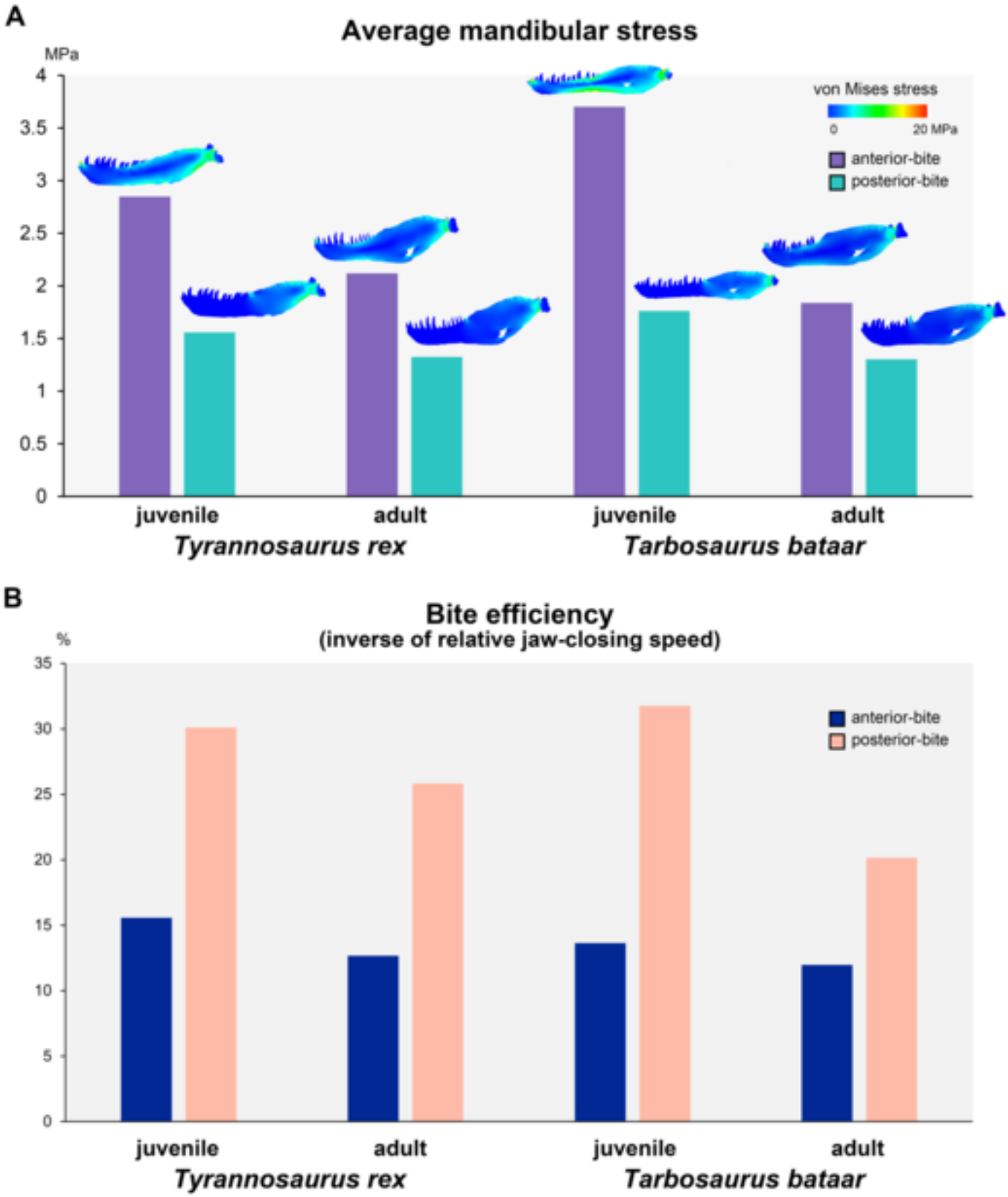

Figure 4

Click here to access/download;Figure;CB_fig4.png

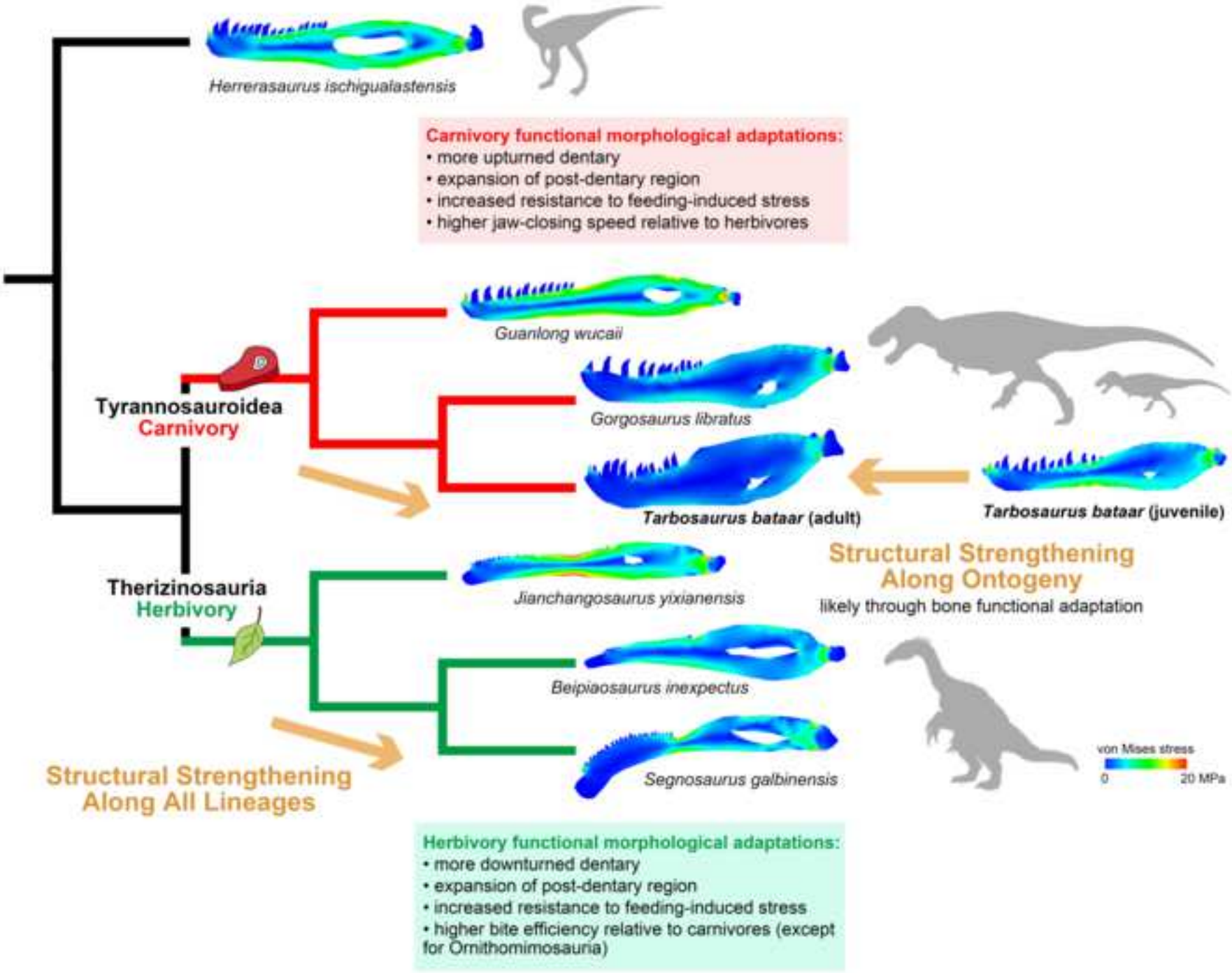

Figure 1

Click here to access/download;Figure;CB_1.png

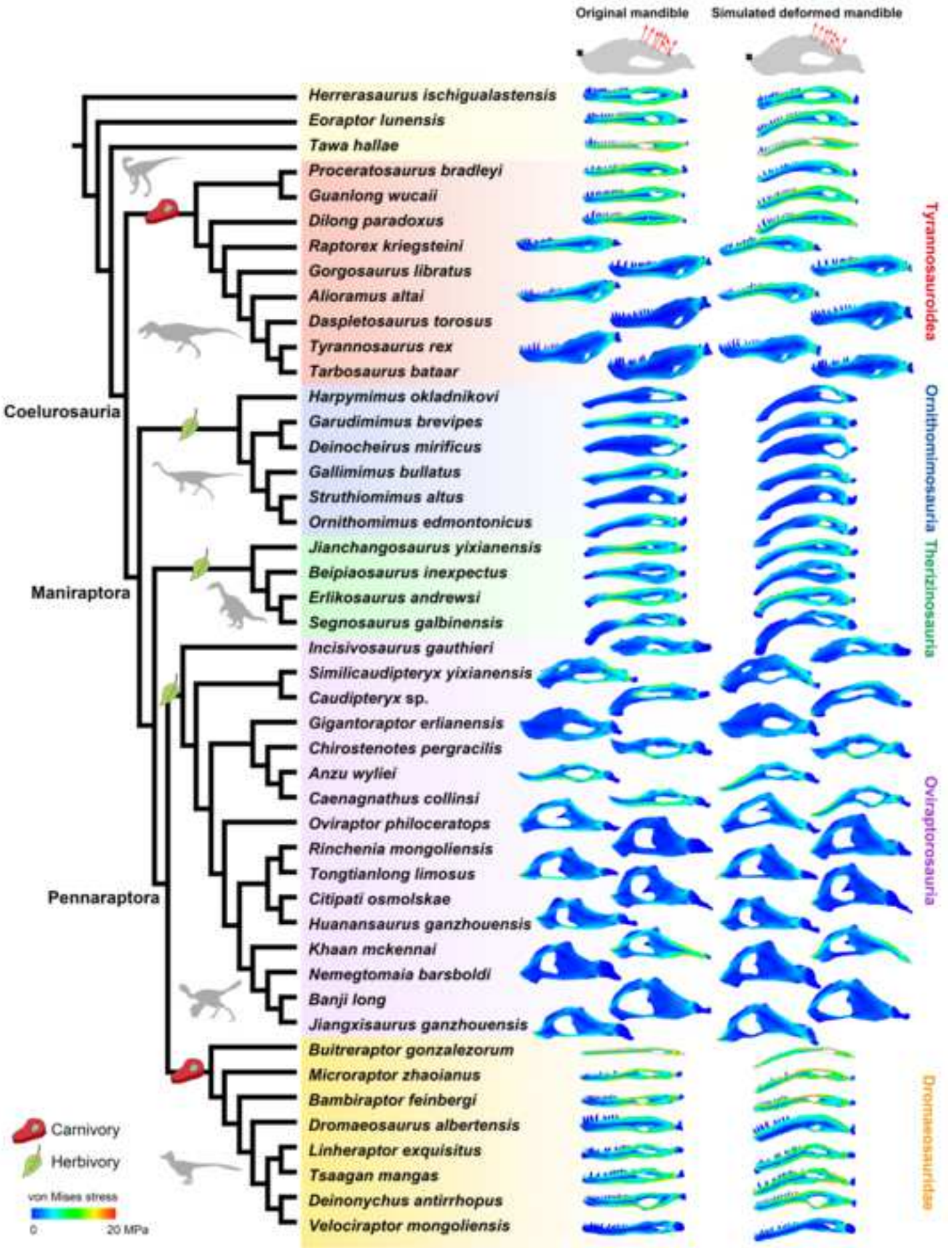

Figure 2

Click here to access/download;Figure;CB_2.png

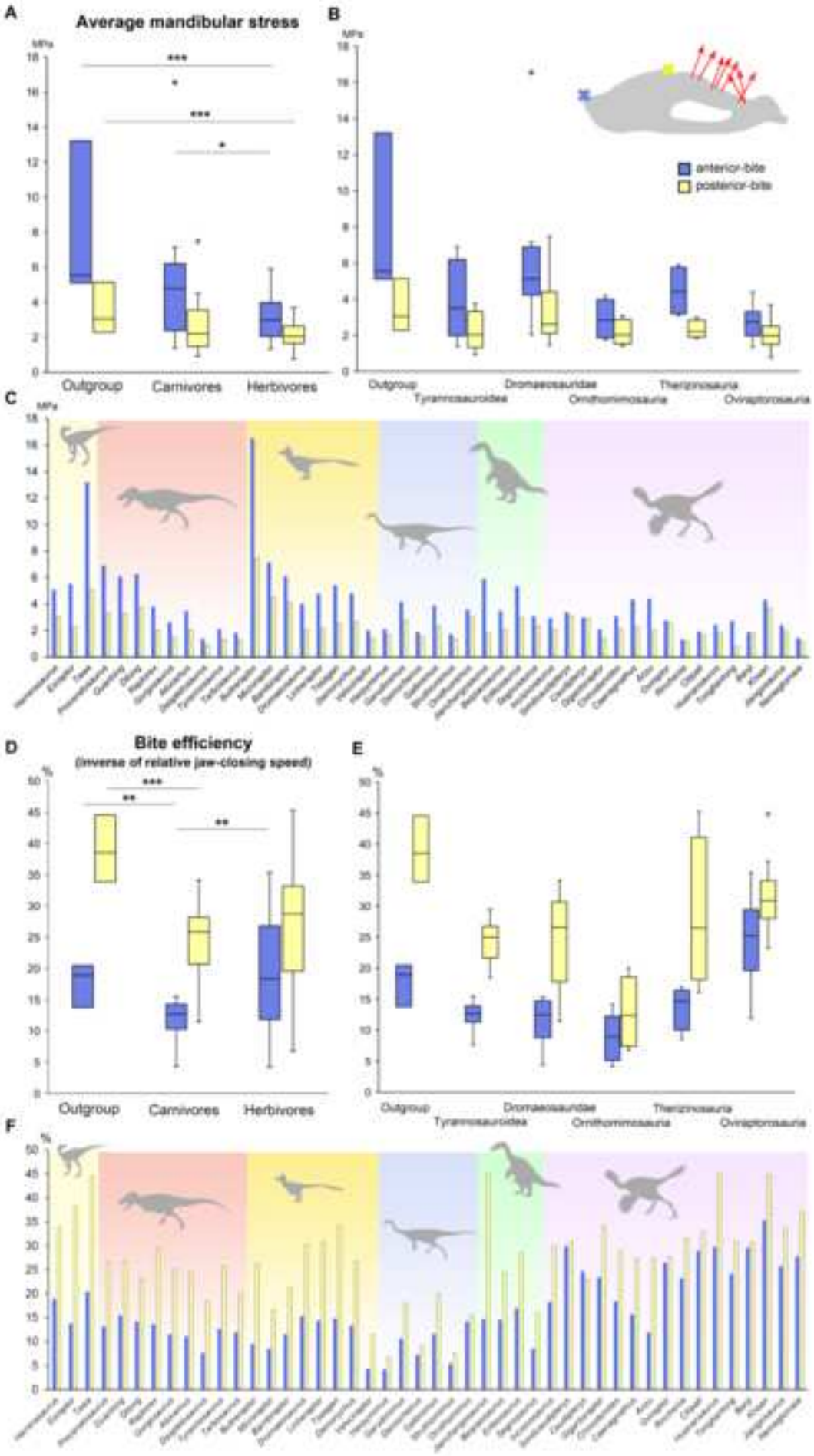

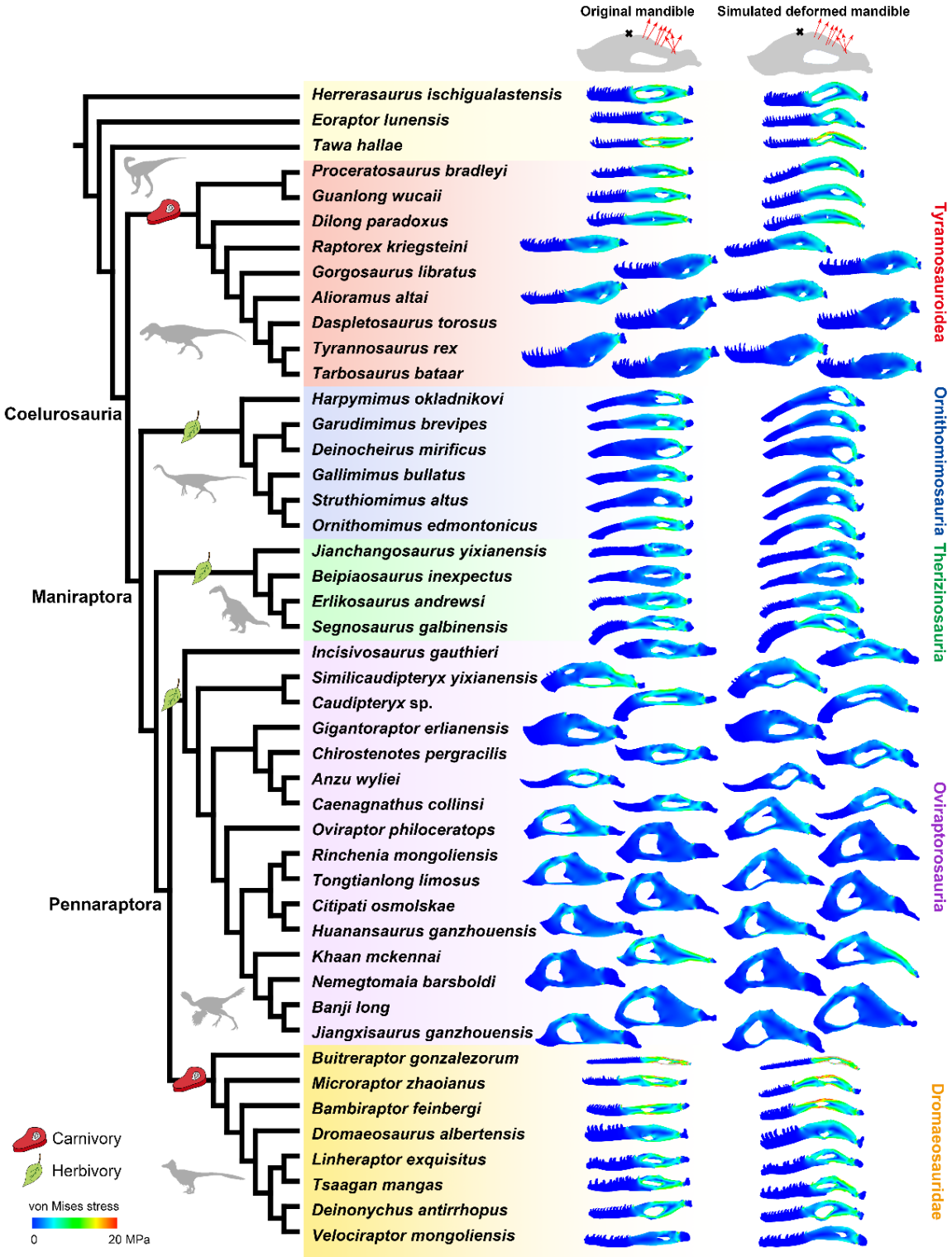

Figure S1. Comparison of von Mises stress plots of non-avialan theropod mandibles under a posterior-bite scenario. Related to Figure 1. Left: original mandible; Right: simulated deformed mandible, showing the deformation (displacement) of the original mandible under loading and the biomechanical performance of this simulated form (see methods). Silhouettes modified from PhyloPic.

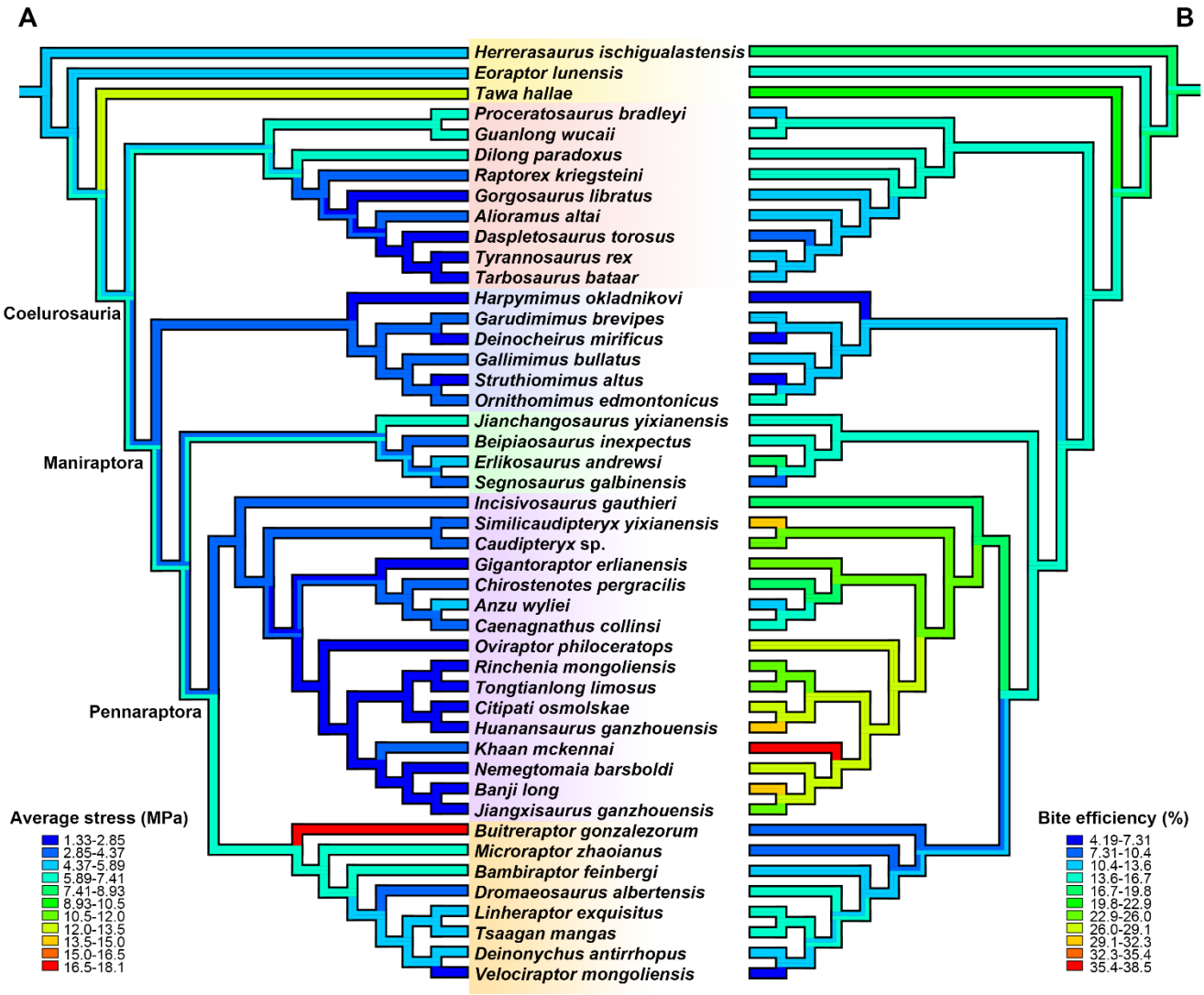

Figure S2. Ancestral state reconstruction of (A) average mandibular stress and (B) bite efficiency of the non-avialan theropods studied under an anterior-bite scenario using linear parsimony. Related to Figures 1 & 2.

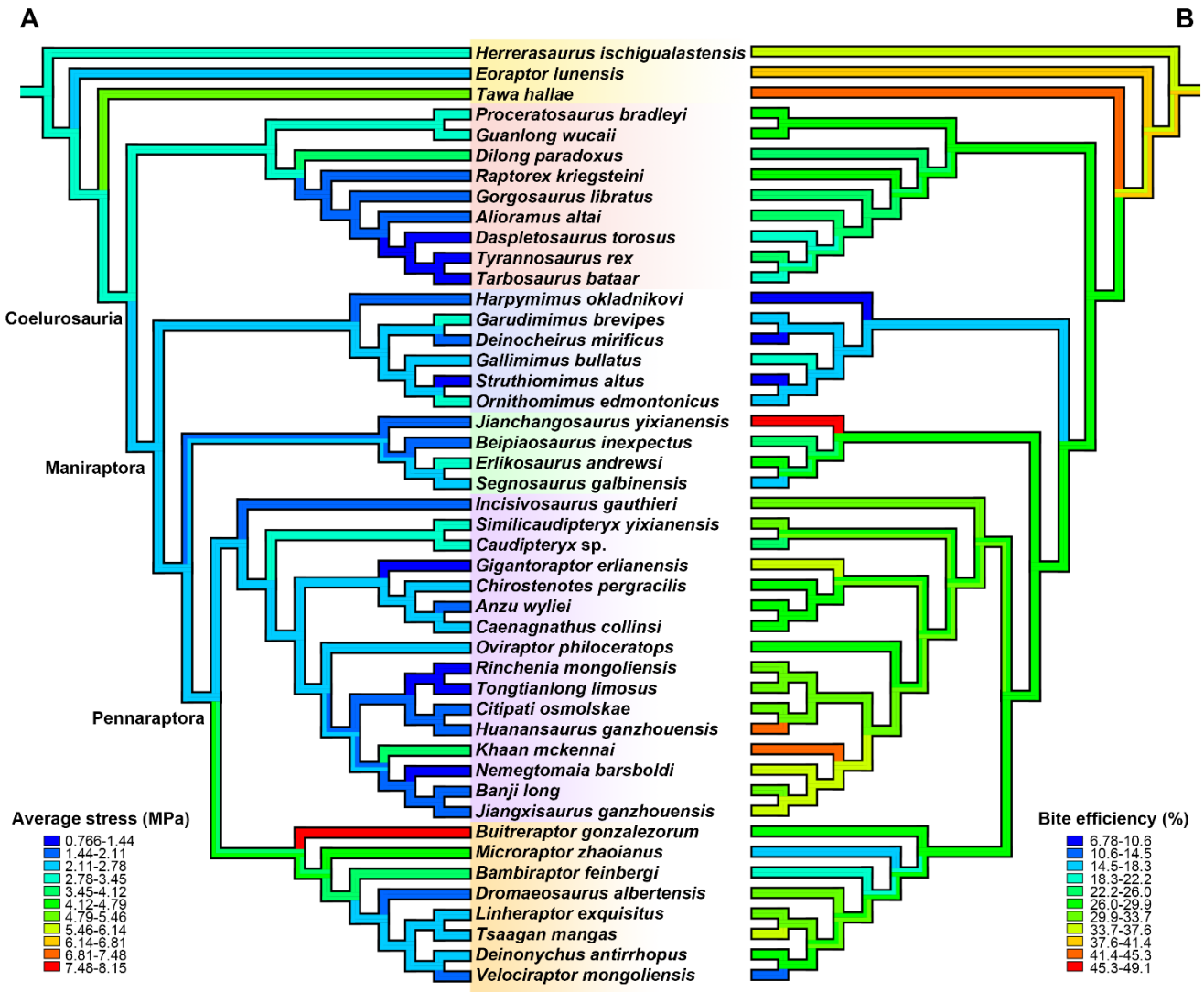

Figure S3. Ancestral state reconstruction of (A) average mandibular stress and (B) bite efficiency of the non-avialan theropods studied under a posterior-bite scenario using linear parsimony. Related to Figures 1 & 2.

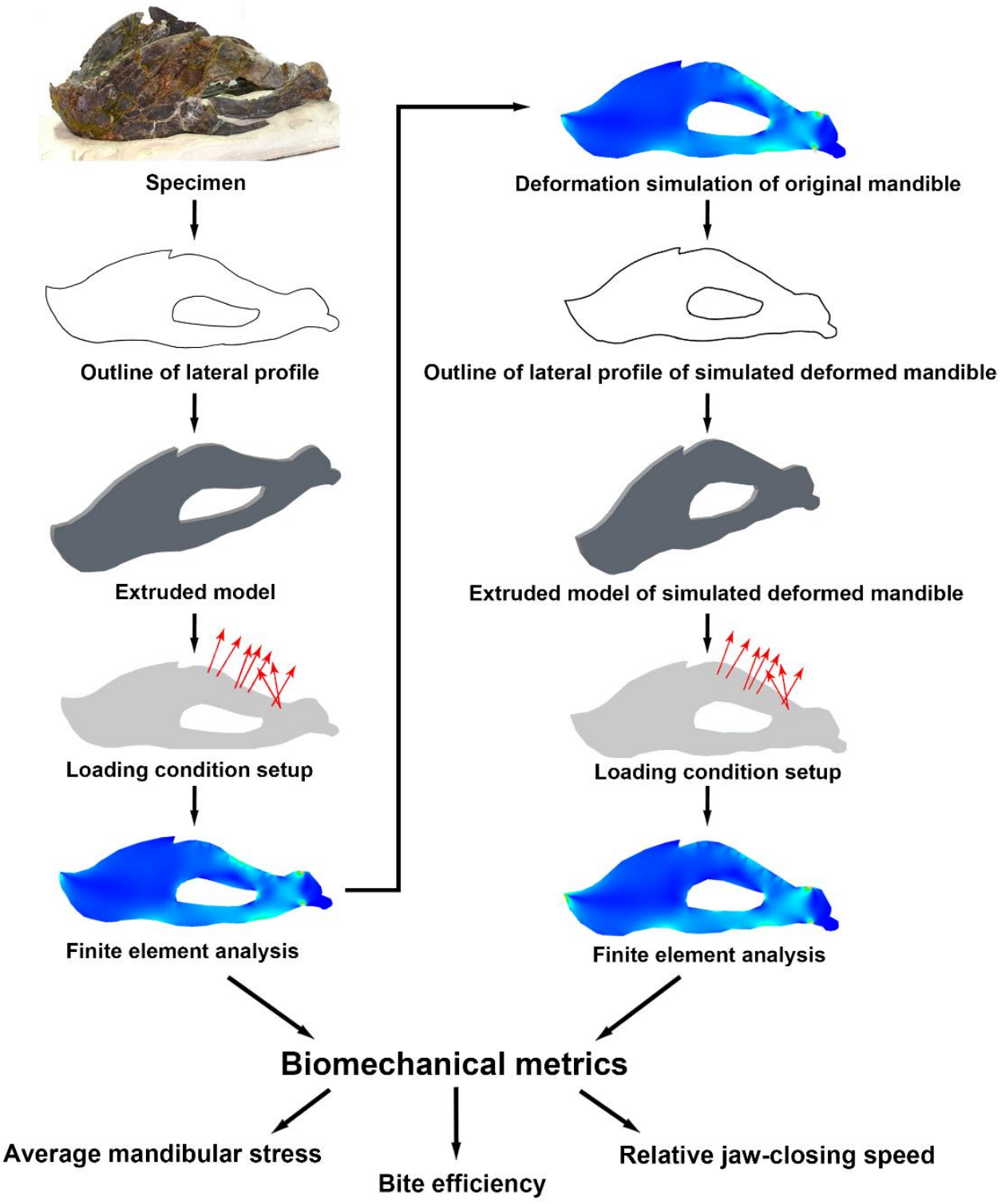

Figure S4. Workflow of the analyses conducted in this study, using the oviraptorosaurian *Gigantoraptor erlianensis* as an example. Related to STAR Methods.

Compared groups (bite location, if specified)	Functional metric	Bite location	p-value	Permutation p (n=99999)	F
Herbivores vs. Carnivores	Average stress	Anterior	0.01164 (0.0007233)	0.00334 (0.00051)	6.975 (13.36)
		Posterior	0.08708 (0.01243)	0.08033 (0.01121)	3.073 (6.838)
	Bite efficiency	Anterior	0.001822 (0.03528)	0.00194 (0.03554)	11.12 (4.74)
		Posterior	0.3436 (0.9471)	0.3463 (0.9476)	0.9182 (0.004449)
Herbivores vs. Outgroup taxa	Average stress	Anterior	5.92e-05 (0.002179)	0.00135 (0.00259)	22.57 (11.47)
		Posterior	0.007595 (0.05286)	0.01484 (0.0565)	8.325 (4.1)
	Bite efficiency	Anterior	0.7628 (0.96)	0.7659 (0.9638)	0.09294 (0.002558)
		Posterior	0.07185 (0.1262)	0.07232 (0.1011)	3.51 (2.49)
Carnivores vs. Outgroup taxa	Average stress	Anterior	0.2151 (0.2166)	0.2075 (0.2207)	1.651 (1.64)
		Posterior	0.4614 (0.5154)	0.4516 (0.5078)	0.5665 (0.4402)
	Bite efficiency	Anterior	0.007785 (0.166)	0.01067 (0.1479)	8.965 (2.084)
		Posterior	0.0006784 (0.01817)	0.00167 (0.01988)	16.78 (6.751)
Herbivores (anterior) vs. Carnivores (posterior)	Average stress	NA	0.4419 (0.000189)	0.4442 (0.00013)	0.6029 (16.83)
	Bite efficiency	NA	0.03259 (0.3117)	0.03346 (0.3125)	4.893 (1.049)
Herbivores (posterior) vs. Carnivores (anterior)	Average stress	NA	0.000167 (0.02996)	1E-05 (0.02829)	17.17 (5.058)
	Bite efficiency	NA	8.577E-07 (0.2461)	1E-05 (0.248)	33.54 (1.384)

Table S1. Differences in mandibular biomechanics between dietary groups of Theropoda shown by Analysis of Variance (ANOVA). Related to Figure 2. Results conducted using the residuals of conducted phylogenetic generalized least square regression (PGLS) are in brackets. Significant p-values ($p < 0.05$) are in red.

	Functional metric	Bite location	p-value	Permutation p (n=99999)	F
Tyrannosauroidea vs. Dromaeosauridae	Average stress	Anterior	0.1441 (0.4547)	0.1231 (0.4671)	2.375 (0.589)
		Posterior	0.1253 (0.5838)	0.1147 (0.6027)	2.635 (0.3135)
	Bite efficiency	Anterior	0.5616 (0.06844)	0.5714 (0.0607)	0.5323 (3.854)
		Posterior	0.9204 (0.3647)	0.9204 (0.3835)	0.01033 (0.8737)
Ornithomimosauria vs. Therizinosauria	Average stress	Anterior	0.08253 (0.115)	0.08103 (0.1241)	3.936 (3.128)
		Posterior	0.7075 (0.9662)	0.7053 (0.966)	0.1513 (0.001908)
	Bite efficiency	Anterior	0.08345 (0.1463)	0.09068 (0.168)	3.908 (2.589)
		Posterior	0.02443 (0.02376)	0.01405 (0.0342)	7.653 (7.753)
Ornithomimosauria vs. Oviraptorosauria	Average stress	Anterior	0.806 (0.1491)	0.804 (0.1495)	0.06191 (2.252)
		Posterior	0.7711 (0.08209)	0.7691 (0.07704)	0.08694 (3.351)
	Bite efficiency	Anterior	9.877e-06 (9.25E-06)	5e-05 (6E-05)	34.33 (34.68)
		Posterior	1.034e-06 (1.272E-06)	1e-05 (4E-05)	47.76 (46.39)
Therizinosauria vs. Oviraptorosauria	Average stress	Anterior	0.0104 (0.00637)	0.00997 (0.00663)	8.181 (9.524)
		Posterior	0.5218 (0.1225)	0.5228 (0.1218)	0.4268 (2.626)
	Bite efficiency	Anterior	0.003208 (0.002979)	0.00311 (0.00376)	11.54 (11.77)
		Posterior	0.3761 (0.3424)	0.3636 (0.336)	0.8236 (0.9509)
Herbivores vs. Tyrannosauroidea	Average stress	Anterior	0.1801 (0.01381)	0.1806 (0.0142)	1.876 (6.764)
		Posterior	0.8558 (0.07423)	0.8558 (0.07378)	0.03353 (3.399)
	Bite efficiency	Anterior	0.02571 (0.3693)	0.02476 (0.3733)	5.457 (0.8285)
		Posterior	0.4414 (0.6752)	0.4431 (0.6865)	0.6073 (0.1787)
Herbivores vs. Dromaeosauridae	Average stress	Anterior	0.001265 (0.002605)	0.00042 (0.00235)	12.5 (10.66)
		Posterior	0.007714 (0.02926)	0.00786 (0.02966)	8.085 (5.209)
	Bite efficiency	Anterior	0.02018 (0.02224)	0.02 (0.02153)	5.977 (5.774)
		Posterior	0.5365 (0.7526)	0.5364 (0.7582)	0.3905 (0.1011)
Outgroup vs. Tyrannosauroidea	Average stress	Anterior	0.0502 (0.1256)	0.0554 (0.1318)	4.954 (2.794)
		Posterior	0.1131 (0.3698)	0.1123 (0.383)	3.017 (0.8819)

	Bite efficiency	Anterior	0.01038 (0.08676)	0.01358 (0.1042)	9.905 (3.606)
		Posterior	0.0002227 (0.0008919)	0.00447 (0.0046)	31.54 (21.73)
Outgroup vs. Dromaeosauridae	Average stress	Anterior	0.6075 (0.4539)	0.7444 (0.4304)	0.2832 (0.6127)
		Posterior	0.9311 (0.7399)	0.9517 (0.7574)	0.007911 (0.1172)
	Bite efficiency	Anterior	0.03624 (0.1099)	0.04382 (0.0903)	6.045 (3.145)
		Posterior	0.01754 (0.05912)	0.02476 (0.05421)	8.421 (4.663)
Carnivores vs. Ornithomimosauria + Therizinosauria	Average stress	Anterior	0.2099 (0.1642)	0.2207 (0.1677)	1.656 (2.054)
		Posterior	0.3376 (0.4399)	0.3648 (0.4462)	0.9557 (0.616)
	Bite efficiency	Anterior	0.4248 (0.3472)	0.421 (0.3498)	0.6584 (0.9178)
		Posterior	0.1143 (0.03064)	0.1158 (0.02883)	2.677 (5.25)
Carnivores vs. Ornithomimosauria + Oviraptorosauria	Average stress	Anterior	0.007506 (0.0001318)	0.00121 (8E-05)	8.001 (18.21)
		Posterior	0.09433 (0.0084)	0.08935 (0.00703)	2.948 (7.753)
	Bite efficiency	Anterior	0.0007945 (0.02802)	0.00118 (0.02762)	13.36 (5.23)
		Posterior	0.3934 (0.8416)	0.3923 (0.8427)	0.7457 (0.04052)
Carnivores vs. Therizinosauria + Oviraptorosauria	Average stress	Anterior	0.02882 (0.001047)	0.01242 (0.00106)	5.198 (12.78)
		Posterior	0.1189 (0.005973)	0.1148 (0.00472)	2.556 (8.569)
	Bite efficiency	Anterior	2.507E-06 (8.69E-05)	1E-05 (2E-05)	31.5 (19.68)
		Posterior	0.002926 (0.02665)	0.0024 (0.02404)	10.23 (5.355)
Outgroup vs. Ornithomimosauria + Therizinosauria	Average stress	Anterior	0.01452 (0.02906)	0.01742 (0.02804)	8.393 (6.293)
		Posterior	0.04057 (0.2136)	0.04518 (0.2192)	5.383 (1.743)
	Bite efficiency	Anterior	0.02972 (0.09825)	0.03881 (0.09395)	6.23 (3.263)
		Posterior	0.01692 (0.03748)	0.02137 (0.04075)	7.904 (5.594)
Outgroup vs. Ornithomimosauria + Oviraptorosauria	Average stress	Anterior	3.757E-05 (0.0006242)	0.00052 (0.00083)	25.88 (15.67)
		Posterior	0.01045 (0.04537)	0.01768 (0.05105)	7.774 (4.478)
	Bite efficiency	Anterior	0.6332 (0.9544)	0.6391 (0.9588)	0.2339 (0.003349)
		Posterior	0.06877 (0.1321)	0.06556 (0.09778)	3.646 (2.437)
	Average stress	Anterior	0.0003458 (0.003176)	0.00297 (0.00518)	18.18 (11.09)

Outgroup vs. Therizinosauria + Oviraptorosauria		Posterior	0.0122 (0.03743)	0.01975 (0.04246)	7.522 (4.936)
	Bite efficiency	Anterior	0.2836 (0.3778)	0.2892 (0.3754)	1.211 (0.8118)
		Posterior	0.1091 (0.1052)	0.1164 (0.1096)	2.8 (2.867)

Table S2. Differences in mandibular biomechanics between theropod clades by Analysis of Variance (ANOVA). Related to Figure 2. Results conducted using the residuals of conducted phylogenetic generalized least square regression (PGLS) are in brackets. Significant p-values ($p < 0.05$) are in red.

	Log average stress (anterior-bite)	Log average stress (posterior-bite)	Log bite efficiency (anterior-bite)	Log bite efficiency (posterior-bite)
Log mandibular length	correlation coefficient = 0.454, p = 0.0301, R^2 = 0.206	correlation coefficient = 0.349, p = 0.0074, R^2 = 0.122	correlation coefficient = -0.555, p = 0.254, R^2 = 0.308	correlation coefficient = -0.404, p = 0.4623, R^2 = 0.163

Table S3. Phylogenetic generalized least square regression between mandibular length and biomechanical characters.

	CDF cumulative distribution function		
	Two sided	**Treatment less than control**	**Treatment greater than control**
Average stress (anterior-bite)	D = 0.52174, p-value = 4.498e-06	D^- = 0.043478, p-value = 0.9167	D^+ = 0.52174, p-value = 3.647e-06
Average stress (posterior-bite)	D = 0.3913, p-value = 0.001565	D^- = 0.043478, p-value = 0.9167	D^+ = 0.3913, p-value = 0.0008731
Bite efficiency (anterior-bite)	D = 0.21739, p-value = 0.2287	D^- = 0.1087, p-value = 0.5807	D^+ = 0.21739, p-value = 0.1137
Bite efficiency (posterior-bite)	D = 0.56522, p-value = 4.065e-07	D^- = 0.086957, p-value = 0.7062	D^+ = 0.56522, p-value = 4.147e-07
Average stress PGLS residuals (anterior-bite)	D = 0.3913, p-value = 0.001565	D^- = 0.043478, p-value = 0.9167	D^+ = 0.3913, p-value = 0.0008731
Average stress PGLS residuals (posterior-bite)	D = 0.17391, p-value = 0.4943	D^- = 0.17391, p-value = 0.2488	D^+ = 0.17391, p-value = 0.2488
Bite efficiency PGLS residuals (anterior-bite)	D = 0.17391, p-value = 0.4943	D^- = 0.17391, p-value = 0.2488	D^+ = 0.086957, p-value = 0.7062
Bite efficiency PGLS residuals (posterior-bite)	D = 0.30435, p-value = 0.02766	D^- = 0.30435, p-value = 0.01411	D^+ = 0.086957, p-value = 0.7062

Table S4. Bootstrap Kolmogorov-Smirnov test comparing the empirical trends and Brownian motion simulated trends of biomechanical characters. The bootstrap p-value tests for the hypothesis that the probability densities for both groups are the same. Significant p-values ($p < 0.05$) are in red.